Full Paper

Design and Synthesis of Quinazolinone Tagged Acridones as Cytotoxic Agents and Their Effects on EGFR Tyrosine Kinase

Yarlagadda Rajesh Babu[1], Mantripragada Bhagavanraju[1], Gade Deepak Reddy[2], Godefridus J. Peters[4], and Velivela V. S. Rajendra Prasad[3,4]

[1] Department of Pharmaceutical Chemistry, Gland Institute of Pharmaceutical Sciences, Narsapur, India
[2] Medicinal Chemistry Research Division, Vishnu Institute of Pharmaceutical Education and Research, Narsapur, India
[3] Department of Pharmaceutical Chemistry, Sitha Institute of Pharmaceutical Sciences, Bachupally, Hyderabad, India
[4] Department of Medical Oncology, VU University Medical Center, Amsterdam, The Netherlands

In a quest for finding potent cytotoxic molecules, we have designed and synthesized a new scaffold by tagging quinazolinones with an acridone moiety. The new acridone-4-carboximide derivatives were evaluated for their cytotoxic potentials against the MCF7 breast cancer cell line and three colon cancer cell lines (LS174T, SW1398, and WiDr). Compound **26** showed relatively potent cytotoxic activity among the derivatives, against all the cell lines tested. Mechanistic studies for the selected derivatives **7**, **8**, **16**, **17**, **25**, and **26** were conducted through *in vitro* EGFR tyrosine kinase inhibition studies. The results indicate that compound **26** has a better EGFR tyrosine kinase inhibitory profile. The *in vitro* EGFR inhibition data was correlated with the cytotoxic properties, and molecular docking studies were performed with regard to the receptor autophosphorylation sites of the protein kinase domain of the EGFR.

Keywords: Acridone / Breast cancer / Docking / EGFR

Received: February 20, 2014; Revised: April 2, 2014; Accepted: April 2, 2014

DOI 10.1002/ardp.201400065

Introduction

Cancer is characterized by a change in controlled mechanisms that manage cell proliferation and differentiation, and is continuing to be a major health problem in developing as well as undeveloped countries [1]. Malignancy is caused by abnormalities in cells, which might be due to inherited genes or caused by exposure to chemicals, radiation, or even infectious agents [2, 3]. The epidermal growth factor receptor (EGFR) is an important receptor tyrosine kinase involved in many critical processes of cancer development, progression and proliferation [4]. EGFR signaling pathway, which acts as a major switch in different signal transduction processes, involves active dimerization of inactive monomer EGFR proteins followed by auto-phosphorylation of kinase domain, which initiates a cascade of intracellular events [5]. Activation of EGFR pathway triggers cell growth, differentiation, motility and adhesion in various cell lineages [6]. In recent years, due to the advances in the chemical and structural biology and signaling transduction studies, EGFR was found to be a highly promising target in oncology that is over-expressed in a significant number of human tumors (e.g. breast, ovarian, colon, and prostate), their expression levels often correlate with vascularity, and is associated with poor prognosis in patients [7–9].

Various substituted quinazoline/quinazolinone derivatives were reported as potent inhibitors of both wild type and mutant EGFR kinase overexpressed in various cancer cell lines. Acridone derivatives such as GF-120918 (acridonecarboxamide), C_{1311} (imidazoacridone derivative) (Figure 1) have very good anticancer activity in model systems [10, 11]. In our previous studies, we have developed diverse series of acridone derivatives with significant cytotoxic profile and also identified an efficient pharmacophore model [12–14]. The present investigation is focused on the design and synthesis of

Correspondence: Dr. Velivela V. S. Rajendra Prasad, Department of Pharmaceutical Chemistry, Sitha Institute of Pharmaceutical Sciences, Bachupally, Hyderabad, India
E-mail: drvvsrp@rediffmail.com
Fax: +91 40 42417772

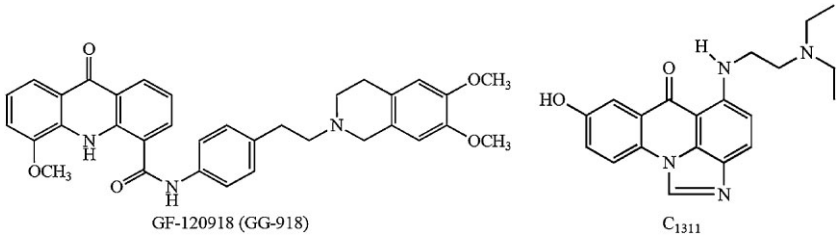

Figure 1. Structures of acridone derivatives (GF-120918 and C_{1311}) showing potential anticancer activity.

quinazolinone linked acridones as potential cytotoxic agents against various cancer cell lines. Mechanistic studies of the designed compounds were elucidated through *in vitro* inhibition of EGFR and the result was correlated with *in silico* data.

Results and discussion

Chemistry

Condensation of anthranilic acid with different acid chlorides was followed by cyclization in the presence of acetic anhydride to give 2-substituted-1,2-dihydro-4*H*-3,1-benzoxazin-4-one derivatives **(IIIa–c)**. Quinazoline derivatives **(IVa–i, Va–i**, and **VIa–i)** were synthesized by the treatment of compounds **(IIIa–c)** with hydrazine, thiourea, and urea, respectively at high temperature up to 2000°C [15, 16]. Physical characterization data of quniazolinone derivatives are listed in Table 1. Further, acridone-4-carboxylic acid (**D**) and its derivatives (**1–27**) were synthesized according to Scheme 1. Initially, acridone-4-carboxylic acid (**D**) was synthesized by the Ullmann condensation of 2-chlorobenzoic acid and anthranilic acid followed by cyclization with polyphosphoric acid at 100°C [17]. The reaction of quinazolines (**IVa–i, Va–i** and **VIa–i**) with acridone-4-carboxylic acid (**D**) in dry toluene in the presence of pyridine, thionylchloride and triethylamine at room temperature led to the corresponding acridone-4-carboxamide derivatives (**1–27**). Structural features and molecular properties of acridone-4-carboxamide derivatives are tabulated in Table 2.

All the compounds were purified by column chromatography and dried under high vacuum up to 15 h. The purified compounds were characterized by ^{1}H NMR, ^{13}C NMR and mass spectral methods. The assignment of protons in all the compounds is fully supported by the integration curves and all the derivatives showed the characteristic chemical shifts for the acridone nucleus. The mass spectra of all the acridone derivatives were analyzed under ESI-MS. Molecular ions were observed either in the form of M+ and M+H in the spectra of these acridone derivatives. From the mass spectral data, it is clear that there is no difference in the fragmentation pattern among the set of acridone series compounds. In general, mass spectral features of these compounds were similar and straight forward. Most of the compounds produce abundant molecular ions in the form of M+H.

Biological activity

Newly synthesized quinazolinone tagged acridone derivatives were evaluated for their *in vitro* cytotoxic activity against different cancer cell lines including the breast cancer cell line MCF7 and the colon cancer cell lines LS174T, SW1398 and WiDr in comparison with the reference drugs mitoxantrone, doxorubicin and 5-fluorouracil by using sulforhodamine B (SRB) assay. The cytotoxic data is presented in Table 3 as IC_{50} concentrations expressed in micromoles (μM). Cytotoxic results indicate that the synthesized molecules displayed marked cytotoxic potentials against cancer cell lines. Among the quinazolinone derivatives screened for the cytotoxic property, bromine-containing compounds (**19–27**) exhibited relatively better cytotoxicity. Among a wide range of distributed hydrophobic and higher electrostatic substitutions, compounds containing phenyl at R and amide linkage (R^1) exhibited marked activity. A phenyl substituted bromoquinazolinone linked to acridone nucleus with an amide linkage (compound **26**) possessed higher cytotoxic potentials than the other compounds against MCF7, LS174T and SW1398 cell lines. Further, selected compounds (**7, 8, 16, 17, 25,** and **26**) were tested for EGFR tyrosine kinase inhibition at a concentration of 10 μM. The results indicate compound **26** displayed the highest EGFR tyrosine kinase inhibition among the selected set of ligands and the inhibition exerted by compound **8** is also above 98%. The percentage EGFR inhibition of the compounds was shown in Table 4. The cytotoxic properties of these molecules showed significant correlation with their corresponding EGFR inhibitory activity.

Molecular docking studies

In silico molecular docking studies were performed to predict the possible mechanistic insights for these novel acridone derivatives against EGFR. Docking of the quinazolinone tagged acridones into the auto-phosphorylation site of the kinase domain of EGFR (PDB ID: 1M17) revealed the possible interacted residues. When the structural features of the molecules were considered all the molecules consist of adequate hydrophobic and hydrophilic regions, which are vital during docking. Nitrogen and oxygen atoms were

Table 1. Physical characterization data of quinazolinone derivatives.

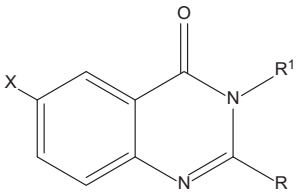

Compound	X	R	R^1	Molecular formula	Molecular weight	Yield (%)	Melting point (°C)
IVa	H	$-CH_3$	$-NH_2$	$C_9H_9N_3O$	175.18	58	201–203
IVb	H	$-C_6H_5$	$-NH_2$	$C_{14}H_{11}N_3O$	237.25	68	207–209
IVc	H	$-C_6H_4CH_3$	$-NH_2$	$C_{15}H_{13}N_3O$	251.28	70	298–300
IVd	I	$-CH_3$	$-NH_2$	$C_9H_8IN_3O$	301.08	45	210–213
IVe	I	$-C_6H_5$	$-NH_2$	$C_{14}H_{10}IN_3O$	363.15	78	205–209
IVf	I	$-C_6H_4CH_3$	$-NH_2$	$C_{15}H_{12}IN_3O$	377.18	70	295–296
IVg	Br	$-CH_3$	$-NH_2$	$C_9H_8BrN_3O$	254.08	40	211–213
IVh	Br	$-C_6H_5$	$-NH_2$	$C_{14}H_{10}BrN_3O$	316.15	76	198–200
IVi	Br	$-C_6H_4CH_3$	$-NH_2$	$C_{15}H_{12}BrN_3O$	330.18	70	290–292
Va	H	$-CH_3$	$-CSNH_2$	$C_{10}H_9N_3OS$	219.26	37	224–226
Vb	H	$-C_6H_5$	$-CSNH_2$	$C_{15}H_{11}N_3OS$	281.33	42	227–229
Vc	H	$-C_6H_4CH_3$	$-CSNH_2$	$C_{16}H_{13}N_3OS$	295.36	40	281–283
Vd	I	$-CH_3$	$-CSNH_2$	$C_{10}H_8IN_3OS$	345.16	40	228–230
Ve	I	$-C_6H_5$	$-CSNH_2$	$C_{15}H_{10}IN_3OS$	407.23	50	220–223
Vf	I	$-C_6H_4CH_3$	$-CSNH_2$	$C_{16}H_{12}IN_3OS$	421.26	53	288–290
Vg	Br	$-CH_3$	$-CSNH_2$	$C_{10}H_8BrN_3OS$	298.16	45	227–229
Vh	Br	$-C_6H_5$	$-CSNH_2$	$C_{15}H_{10}BrN_3OS$	360.23	40	230–233
Vi	Br	$-C_6H_4CH_3$	$-CSNH_2$	$C_{16}H_{12}BrN_3OS$	374.25	50	287–289
VIa	H	$-CH_3$	$-CONH_2$	$C_{10}H_9N_3O_2$	203.19	33	221–223
VIb	H	$-C_6H_5$	$-CONH_2$	$C_{15}H_{11}N_3O_2$	265.26	26	216–218
VIc	H	$-C_6H_4CH_3$	$-CONH_2$	$C_{16}H_{13}N_3O_2$	279.29	50	310–312
VId	I	$-CH_3$	$-CONH_2$	$C_{10}H_8IN_3O_2$	329.09	40	224–226
VIe	I	$-C_6H_5$	$-CONH_2$	$C_{15}H_{10}IN_3O_2$	391.16	35	218–220
VIf	I	$-C_6H_4CH_3$	$-CONH_2$	$C_{16}H_{12}IN_3O_2$	405.19	50	290–294
VIg	Br	$-CH_3$	$-CONH_2$	$C_{10}H_8BrN_3O_2$	282.09	45	210–212
VIh	Br	$-C_6H_5$	$-CONH_2$	$C_{15}H_{10}BrN_3O_2$	344.16	39	220–223
VIi	Br	$-C_6H_4CH_3$	$-CONH_2$	$C_{16}H_{12}BrN_3O_2$	358.19	40	290–292

positioned appropriately in the 3D spatial arrangement of every ligand that enhances the possibilities of better hydrogen bonding with protein residues. In the current investigations structural insights for protein interactions of compounds **7, 8, 16, 17, 25,** and **26** are elucidated. Docking result of the dataset compounds were listed in Table 5. Docking of compound **8, 17,** and **16** were performed into the receptor auto-phosphorylation site, which is a prominent site for most of the kinase inhibitors. This revealed the protein ligand interaction map with all the possible hydrophilic and hydrophobic interactions. Compound **26** exhibited one hydrogen bond interaction (nitrogen of quinazoline nucleus) with Lys721 (2.004 Å). It also displayed potential hydrophobic interactions with the residues present in the binding pocket and this might be the reason for its higher dock score (−7.015). Binding interactions of compound **26** with EGFR is shown in Figure 2. Compound **8** did not display significant hydrogen bond interaction (Figure 3), but it has greater hydrophobic interactions and this could possibly explain its higher dock score (−6.820) and enhanced *in vitro* EGFR inhibition among the molecules studied. Other residues such as Met769 and Asp831 have shown hydrogen bond interacted with compounds **7** and **25** and oxygen atom of amide linkage in compound **25** acts as H-bond acceptor. Larger tricyclic acridone nucleus and quinazolinone moiety extends their contribution in docking with their higher hydrophobic nature.

Conclusion

Two potent moieties acridone and quinazolinone individually have shown significant cytotoxic properties. In the present investigation we designed a new scaffold by tagging acridone with different quinazolinones through amide bridge, with the aim to enhance the cytotoxicity. The molecules were evaluated for their cytotoxic activity against breast cancer cells and three types of colon cancer cells. The results indicate

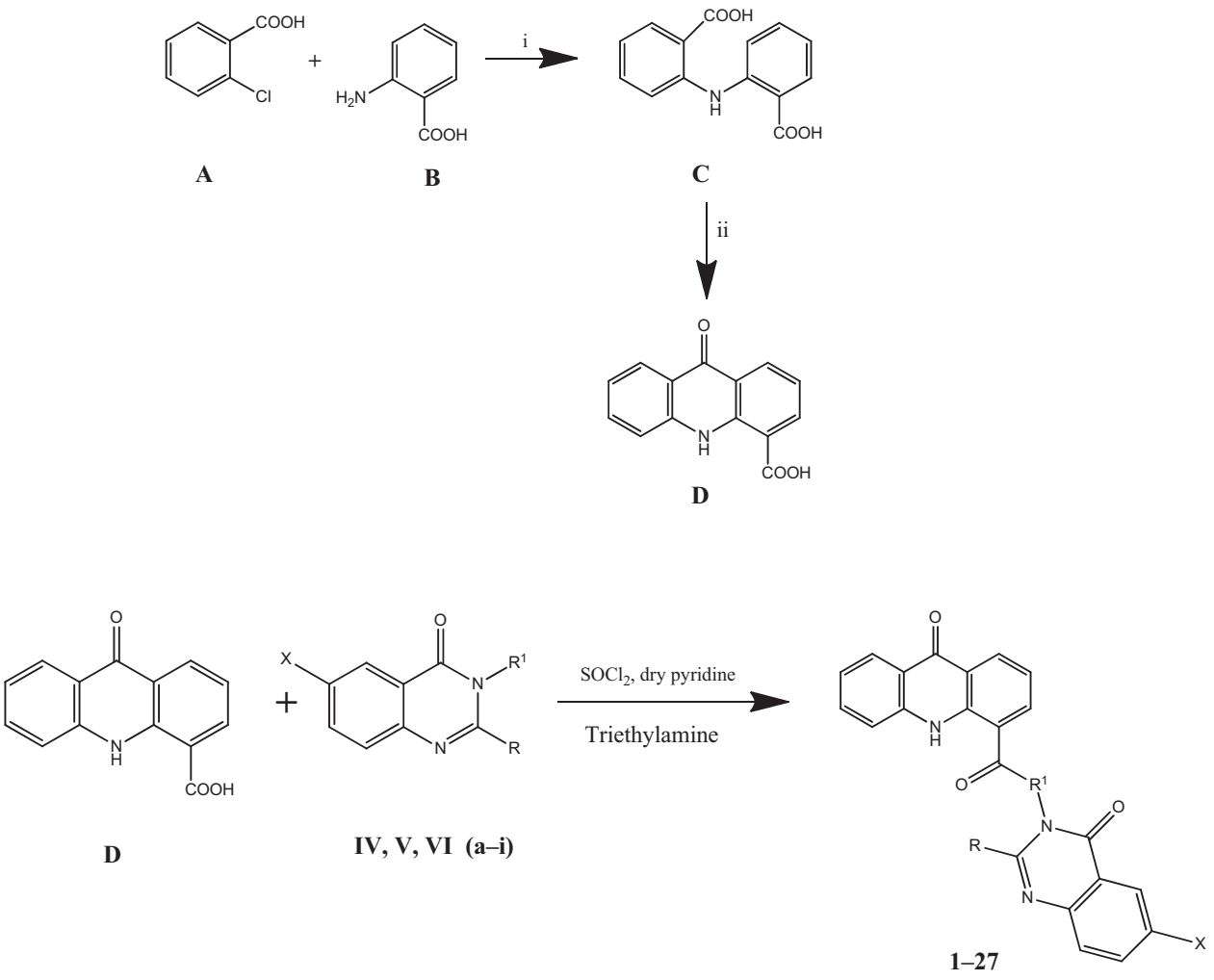

Scheme 1. Synthesis of acridone-4-carboxamide derivatives. Reagents and conditions: (i) Cu, K_2CO_3, Isoamyl alcohol, reflux for 6–8 h, 160°C (ii) PPA, 100°C, 3 h.

that compound **26** showed a broad spectrum and potent antitumor activity against MCF7 cells with IC_{50} of 2.9 μM. As breast cancer cells are known to overexpress EGFR, which leads to enhanced activation of the EGFR pathway involved in cell proliferation, various *in silico* and *in vitro* EGFR interaction studies further support the understanding of cytotoxic selectivity over MCF-7 cell line and thereby help to design new molecules. Results of the molecular docking studies support the strong inhibitory activity of compounds **8, 17**, and **26**. Results of this study help in understanding the interaction between the ligands and EGFR protein kinase in detail and assist in the design and development of new EGFR inhibitors.

Experimental

All chemicals and solvents were supplied by Sigma–Aldrich, India and S.D. Fine Chemicals Limited, Mumbai. Reactions were monitored by TLC and compounds were purified by using column chromatography with silica gel Merck Grade 60 (230–400 mesh, 60; Merck, Germany). Melting points were recorded on a Tempirol hot-stage with microscope (AGA International, Ambala City, Haryana, India) and are uncorrected. Elemental analysis was performed and found values are within 0.4% of theoretical values unless otherwise noted. ^{1}H NMR spectra were recorded in DMSO-d_6 solution in a 5-mm tube on a Bruker drx 500 Fourier transform spectrometer (Bruker Bioscience, USA) and TMS was used as internal standard. Chemical shifts are expressed as δ (ppm) values. The spectrometer was internally locked to deuterium frequency of the solvent. To obtain molecular weight information, acridone derivatives were analyzed by ESI-MS spectrometry. Collision-induced dissociation (CID) spectra were acquired in the positive ion mode on a MDS Sciex (Concord, Ont., Canada) API 4000 triple quadrupole mass spectrometry with direct infusion of each acridone at a concentration of 10 μM in 50% methanol, at flow rate of 25 μL/min. The instrument was operated with a spray voltage of 5.5 kV, a declustering potential of 50 eV, a source temperature of 100°C, a GSI value of 50 and the

Table 2. Physical characterization data of acridone derivatives.

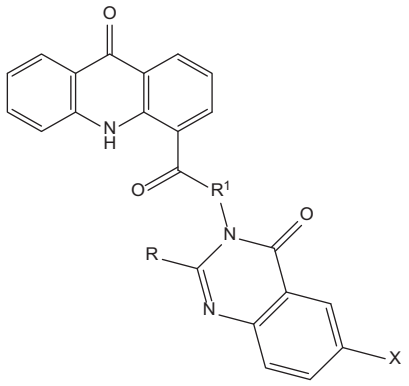

Compound	X	R	R^1	Molecular formula	Molecular weight	Yield (%)	Melting point (°C)	Log p
1	H	$-CH_3$	–NH	$C_{23}H_{16}N_4O_3$	396.39	59	272	2.98
2	H	$-C_6H_5$	–NH	$C_{28}H_{18}N_4O_3$	458.46	48	265	4.87
3	H	$-C_6H_4CH_3$	–NH	$C_{29}H_{20}N_4O_3$	472.49	51	275	5.36
4	H	$-CH_3$	–NHCS	$C_{24}H_{16}N_4O_3S$	440.47	45	204	3.63
5	H	$-C_6H_5$	–NHCS	$C_{29}H_{18}N_4O_3S$	502.54	35	278	5.52
6	H	$-C_6H_4CH_3$	–NHCS	$C_{30}H_{20}N_4O_3S$	516.57	37	288	6.01
7	H	$-CH_3$	–NHCO	$C_{24}H_{16}N_4O_4$	424.40	64	282	3.08
8	H	$-C_6H_5$	–NHCO	$C_{29}H_{18}N_4O_4$	486.47	38	247	4.98
9	H	$-C_6H_4CH_3$	–NHCO	$C_{30}H_{20}N_4O_4$	500.50	41	267	5.47
10	I	$-CH_3$	–NH	$C_{23}H_{15}IN_4O_3$	522.29	55	283	4.33
11	I	$-C_6H_5$	–NH	$C_{28}H_{17}IN_4O_3$	584.36	40	271	6.23
12	I	$-C_6H_4CH_3$	–NH	$C_{29}H_{19}IN_4O_3$	598.39	46	270	6.72
13	I	$-CH_3$	–NHCS	$C_{24}H_{15}IN_4O_3S$	566.37	40	224	4.98
14	I	$-C_6H_5$	–NHCS	$C_{29}H_{17}IN_4O_3S$	628.44	40	259	6.88
15	I	$-C_6H_4CH_3$	–NHCS	$C_{30}H_{19}IN_4O_3S$	642.47	45	283	7.37
16	I	$-CH_3$	–NHCO	$C_{24}H_{15}IN_4O_4$	550.30	70	289	4.44
17	I	$-C_6H_5$	–NHCO	$C_{29}H_{17}IN_4O_4$	612.37	45	238	6.34
18	I	$-C_6H_4CH_3$	–NHCO	$C_{30}H_{19}IN_4O_4$	626.40	40	248	6.82
19	Br	$-CH_3$	–NH	$C_{23}H_{15}BrN_4O_3$	475.29	51	268	3.81
20	Br	$-C_6H_5$	–NH	$C_{28}H_{17}BrN_4O_3$	537.36	45	269	5.7
21	Br	$-C_6H_4CH_3$	–NH	$C_{29}H_{19}BrN_4O_3$	551.39	55	289	6.19
22	Br	$-CH_3$	–NHCS	$C_{24}H_{15}BrN_4O_3S$	519.37	50	219	4.45
23	Br	$-C_6H_5$	–NHCS	$C_{29}H_{17}BrN_4O_3S$	581.44	45	269	6.35
24	Br	$-C_6H_4CH_3$	–NHCS	$C_{30}H_{19}BrN_4O_3S$	595.47	50	276	6.84
25	Br	$-CH_3$	–NHCO	$C_{24}H_{15}BrN_4O_4$	503.30	65	293	3.91
26	Br	$-C_6H_5$	–NHCO	$C_{29}H_{17}BrN_4O_4$	565.37	57	245	5.81
27	Br	$-C_6H_4CH_3$	–NHCO	$C_{30}H_{19}BrN_4O_4$	579.40	45	270	6.29

curtain gas set at 10. Ultra-pure nitrogen was used as both curtain gas and collision gas. MS/MS spectra of the protonated molecule of each drug were acquired and multiple reaction monitoring (MRM) transition for important fragments were monitored as the collision energy was ramped from 5–100 V (step size 0.5 V). The data for the fragment-ion curves represent an average of five consecutive experiments.

Chemistry

*General method for the synthesis of 2-acetamidobenzoic acid (**IIa**)*

Quinazolinone derivatives were synthesized by using previously described method shown in Scheme 2 [15, 16]. Anthranilic acid (6.85 g, 0.05 moles), acetyl chloride (5.1 mL, 0.05 moles) and pyridine (4 mL) were stirred at room temperature in 50 mL of dry toluene for 6 h. The solvent was removed under reduced pressure, and the obtained residue was poured onto crushed ice. Product obtained was filtered, washed with water, dried at room temperature and recrystallized from a mixture of chloroform and ethyl acetate.

Yield: 81%;mp: 165–167°C; ^{1}H NMR (DMSO-d_6) δ ppm: 2.04 (s, 3H, CH_3), 7.40–8.4 (m, 4H, Ar–H), 9.23 (s, 1H, –NHCO), 11.1 (s, 1H, OH); ^{13}C NMR (DMSO-d_6) δ: 177.4, 176.3, 139.7, 138.3, 133.5, 131.9, 129.5, 128.5, 23.6; ESI-MS (*m*/*z*, %): 179.07 (100).

*2-Benzamidobenzoic acid (**IIb**)*

Yield: 86%;mp: 270–272°C; ^{1}H NMR (DMSO-d_6) δ ppm: 7.40–8.08 (m, 9H, Ar–H), 9.15 (s, 1H, –NHCO), 11.30 (s, 1H, OH); ^{13}C NMR (DMSO-d_6) δ: 178.3, 177.7, 141.5, 139.3, 134.7, 132.3, 129.3, 127.5, 126.4, 124.7, 123.4, 120.9; ESI-MS (*m*/*z*, %): 241.07 (95).

Table 3. *In vitro* cytotoxic activity of the compounds against sensitive and resistant human cancer cell lines in comparison with reference drugs doxorubicin (DX), mitoxantrone (MR), and 5-fluorouracil (5-FU).

	Cell lines[a]/IC_{50} (μM) ± SEM[b]			
Compound	**MCF7**	**LS174T**	**SW1398**	**WiDr**
1	ND	6.5 ± 2.2	13.8 ± 3.2	12.9 ± 1.6
2	8.1 ± 2.0	ND	ND	ND
6	11.6 ± 1.3	ND	ND	13.2 ± 2.9
7	6.5 ± 1.0	8.8 ± 1.1	11.3 ± 1.2	10.7 ± 1.8
8	3.1 ± 2.1	6.1 ± 1.8	7.9 ± 3.1	9.8 ± 1.4
9	14.8 ± 4.2	8.0 ± 2.2	7.1 ± 4.2	10.5 ± 2.9
10	6.9 ± 1.9	5.4 ± 1.2	11.9 ± 3.2	14.1 ± 1.8
11	10.2 ± 1.8	13.2 ± 1.3	10.1 ± 3.1	11.2 ± 2.4
12	13.2 ± 2.5	ND	ND	ND
15	9.8 ± 1.6	ND	ND	ND
16	5.6 ± 1.2	11.2 ± 1.0	16.0 ± 3.1	11.4 ± 1.1
17	3.5 ± 2.0	4.4 ± 1.1	9.8 ± 2.0	8.1 ± 1.9
18	12.6 ± 3.0	11.3 ± 2.0	8.9 ± 2.2	16.9 ± 2.6
19	6.9 ± 1.7	10.6 ± 2.0	15.5 ± 2.2	18.2 ± 2.2
20	7.9 ± 2.3	10.3 ± 1.8	14.6 ± 3.4	9.4 ± 2.3
22	11.5 ± 3.2	ND	ND	ND
23	8.3 ± 1.5	12.0 ± 2.1	18.0 ± 2.1	13.1 ± 2.4
25	5.4 ± 1.1	5.5 ± 1.3	9.2 ± 1.4	16.0 ± 1.5
26	2.9 ± 1.2	6.2 ± 1.5	6.0 ± 2.0	11.8 ± 2.2
27	11.5 ± 3.0	17.2 ± 3.0	10.5 ± 2.2	11.4 ± 2.1
DX	0.098	–	–	–
MR	0.001	–	–	–
5-FU	–	1.2 ± 0.3	1.8 ± 0.4	2.1 ± 0.7

ND, not determined, each value represents the mean of triplicate experiments.
[a] MCF7 breast cancer cell line, LS174T, SW1398 and WiDr are colon cancer cells.
[b] SEM, standard error of the mean.

Table 4. EGFR tyrosine kinase assay of acridone derivatives at single dose.

Compound	**% Inhibition of EGFR tyrosine kinase[a]**
7	80
8	98
16	86
17	91
25	90
26	100
Gefitinib[b]	100
Staurosporine[c]	98

[a] EGFR tyrosine kinase inhibition at concentration of 10 μM.
[b] Percentage inhibition measured at the concentration 10 μM.
[c] Percentage inhibition measured at the concentration 1 μM.

Table 5. Protein ligand interactions of quinazoline tagged acridone derivatives.

Compound	**Dock score**	**No. of hydrogen bonds**	**Interacted protein residues**	**H-bond distance (Å)**
7	−4.286	2	Lys721, Met769	2.103, 1.904
8	−6.820	–	–	–
16	−5.221			–
17	−6.962	1	Lys721	2.252
25	−5.445	2	Lys721, Asp831	1.830, 2.213
26	−7.015	1	Lys721	2.004

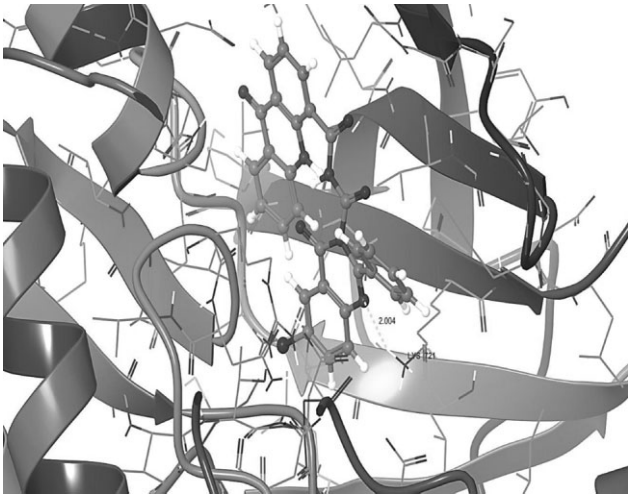

Figure 2. Protein ligand interactions of compound **26** with the kinase EGFR kinase domain.

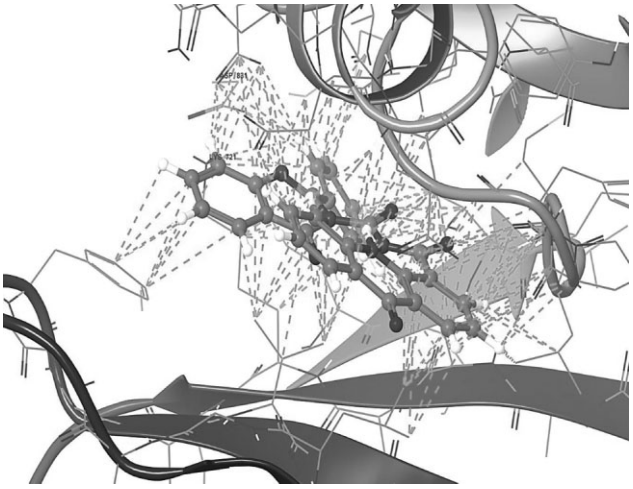

Figure 3. Hydrophobic interaction (dotted lines) of compound **8** at the binding pocket of EGFR kinase domain.

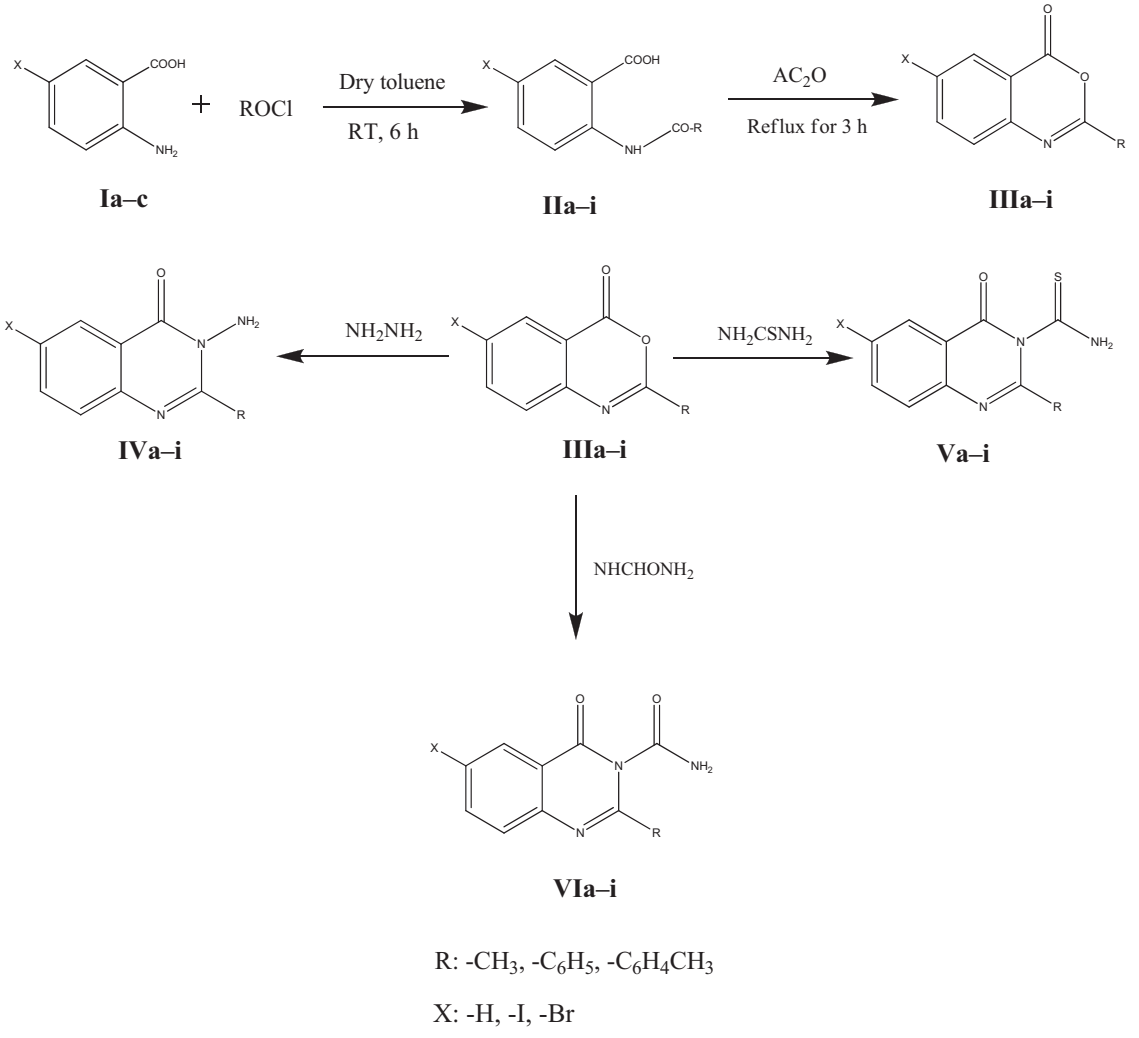

Scheme 2. Synthesis of quinazolinone derivatives.

*2-(4-Methylbenzamido)benzoic acid (**IIc**)*

Yield: 76%; mp: 291–293°C; ^{1}H NMR (DMSO-d_6) δ ppm: 2.34 (s, 3H, CH_3), 7.40–8.3 (m, 8H, Ar–H), 9.73 (s, 1H, NHCO), 11.2 (s, 1H, OH); ^{13}C NMR (DMSO-d_6) δ: 178.7, 177.3, 139.6, 138.4, 133.7, 131.9, 129.5, 128.3, 125.4, 124.7, 123.5, 121.2, 28.3; ESI-MS (*m*/*z*, %): 255.09 (90).

*General method for the synthesis of 2-methyl-4H-benzo[d]-[1,3]oxazin-4-one (**IIIa**)*

2-Acetamidobenzoic acid (1.79 g, 0.01 moles) was heated under reflux in 10 mL of acetic anhydride under anhydrous conditions for about 3 h. The reaction mixture was transferred into ice-cold water and the separated solid was collected by filtration, dried and recrystallized from ethanol.

Yield: 75%; mp: 190–192°C; ^{1}H NMR (DMSO-d_6) δ ppm: 2.47 (s, 3H, CH_3), 7.66–8.21 (m, 4H, Ar–H); ^{13}C NMR (DMSO-d_6) δ: 177.4, 142.3, 139.6, 137.3, 133.7, 131.3, 129.1, 128.7, 23.9; ESI-MS (*m*/*z*, %): 161.16 (100).

*2-Phenyl-4H-benzo[d][1,3]oxazin-4-one (**IIIb**)*

Yield: 79%; mp: 211–213°C; ^{1}H NMR (DMSO-d_6) δ ppm: 7.57–8.21 (m, 9H, Ar–H); ^{13}C NMR (DMSO-d_6) δ: 178.3, 141.6, 139.4, 136.2, 133.6, 132.7, 128.5, 127.3, 125.6, 124.3, 123.6, 121.3; ESI-MS (*m*/*z*, %): 223.06 (100).

*2-(p-Tolyl)-4H-benzo[d][1,3]oxazin-4-one (**IIIc**)*

Yield: 81%; mp: 270–272°C; ^{1}H NMR (DMSO-d_6) δ ppm: 2.34 (s, 3H, CH_3), 7.28–8.41 (m, 8H, Ar–H); ^{13}C NMR (DMSO-d_6) δ: 179.7, 141.3, 139.5, 138.1, 134.7, 132.9, 128.5, 127.3, 125.2, 124.3, 123.7, 121.3, 28.1; ESI-MS (*m*/*z*, %): 237.08 (80).

*General method for the synthesis of 3-amino-2-methylquinazolin-4(3H)-one (**IVa**)*

2-Methyl-4*H*-benzo[d][1,3]oxazin-4-one **(IIIa)** (1.61 g, 0.01 moles) was heated to melt, then excess of hydrazine hydrate was added. The mixture was fused together at 200°C in an oil bath for 1 h.

The separated solid was cooled, collected by filtration, washed with water, dried and purified by column chromatography (methanol/chloroform/water, 10:2:1).

Yield: 58%; mp: 201–203°C; ^{1}H NMR (DMSO-d_6) δ ppm: 2.57 (s, 3H, CH_3), 5.80 (s, 2H, NH_2), 7.45–8.11 (m, 4H, Ar-H); ^{13}C NMR (DMSO-d_6) δ: 178.1, 142.4, 139.7, 137.3, 133.7, 131.3, 129.3, 128.7, 23.7; ESI-MS (*m*/*z*, %): 175.03 (100).

*3-Amino-2-phenylquinazolin-4(3H)-one (**IVb**)*

Yield: 68%; mp: 207–209°C; ^{1}H NMR (DMSO-d_6) δ ppm: 5.66 (s, 2H, $-NH_2$), 7.49–8.20 (m, 9H, Ar–H); ^{13}C NMR (DMSO-d_6) δ: 178.1, 141.3, 139.6, 136.3, 133.7, 132.5, 128.3, 127.3, 125.8, 124.7, 121.6, 120.3; ESI-MS (*m*/*z*, %): 237.09 (100).

*3-Amino-2-(p-tolyl)quinazolin-4(3H)-one (**IVc**)*

Yield: 70%; mp: 298–300°C; ^{1}H NMR (DMSO-d_6) δ ppm: 2.34 (s, 3H, CH_3), 4.93 (s, 2H, $-NH_2$), 7.28–8.04 (m, 8H, Ar–H); ^{13}C NMR (DMSO-d_6) δ: 178.7, 141.3, 139.3, 137.1, 133.7, 132.4, 128.7, 127.3, 125.6, 124.3, 123.1, 121.7, 28.3; ESI-MS (*m*/*z*, %): 251.11 (90).

*Synthesis of 2-methyl-4-oxoquinazoline-3(4H)-carbothioamide (**Va**)*

Equimolar quantities of 2-methyl-4*H*-benzo[d][1,3]oxazin-4-one (**IIIa**) (1.61 g, 0.01 moles) and thiourea (0.76 g, 0.01 moles) were fused together at 200°C in an oil bath for 1 h. The reaction mixture was cooled; the precipitate was collected by filtration, dried and crystallized from ethanol.

Yield: 37%; mp: 224–226°C; ^{1}H NMR (DMSO-d_6) δ ppm: 2.34 (s, 3H, CH_3), 5.56 (s, 2H, $-NH_2$), 7.42–8.08 (m, 4H, Ar–H); ^{13}C NMR (DMSO-d_6) δ: 178.3, 176.3, 142.6, 139.1, 137.4, 133.3, 131.5, 129.3, 128.9, 23.3; ESI-MS (*m*/*z*, %): 219.05 (100).

*4-Oxo-2-phenylquinazoline-3(4H)-carbothioamide (**Vb**)*

Yield: 42%; mp: 227–229°C; ^{1}H NMR (DMSO-d_6) δ ppm: 5.84 (s, 2H, $-NH_2$), 7.50–8.19 (m, 9H, Ar–H); ^{13}C NMR (DMSO-d_6) δ: 178.7, 177.3, 141.1, 138.6, 136.7, 134.7, 132.3, 129.3, 127.9, 125.3, 124.1, 122.6, 121.3; ESI-MS (*m*/*z*, %): 281.06 (35).

*4-Oxo-2-(p-tolyl)quinazoline-3(4H)-carbothioamide (**Vc**)*

Yield: 40%; mp: 281–283°C; ^{1}H NMR (DMSO-d_6) δ ppm: 3.24 (s, 3H, CH_3), 5.86 (s, 2H, NH_2), 7.31–8.24 (m, 8H, Ar–H); ^{13}C NMR (DMSO-d_6) δ: 178.7, 176.3, 141.5, 139.7, 137.3, 135.7, 133.4, 129.7, 127.5, 125.8, 124.9, 123.3, 121.9, 27.3; ESI-MS (*m*/*z*, %): 295.08 (60).

*Synthesis of 2-methyl-4-oxoquinazoline-3(4H)-carboxamide (**VIa**)*

Equimolar quantities of 2-methyl-4*H*-benzo[d][1,3]oxazin-4-one (**IIIa**) (1.61 g, 0.01 moles) and urea (0.01 moles) were fused together at 200°C in an oil bath for 1 h. The reaction mixture was cooled; the precipitate was collected by filtration, dried and crystallized from ethanol.

Yield: 33%; mp: 221–223°C; ^{1}H NMR (DMSO-d_6) δ ppm: 2.34 (s, 3H, CH_3), 5.84 (s, 2H, NH_2), 7.20–8.12 (m, 4H, Ar–H); ^{13}C NMR (DMSO-d_6) δ: 178.7, 177.3, 141.6, 139.3, 137.5, 133.9, 131.3, 129.7, 128.1, 25.3; ESI-MS (*m*/*z*, %): 203.07 (60).

*4-Oxo-2-phenylquinazoline-3(4H)-carboxamide (**VIb**)*

Yield: 26%; mp: 216–218°C; ^{1}H NMR (DMSO-d_6) δ ppm: 5.83 (s, 2H, NH_2), 7.52–8.34 (m, 9H, Ar–H); ^{13}C NMR (DMSO-d_6) δ: 178.1, 177.4, 141.3, 138.9, 136.3, 135.7, 133.3, 129.9, 126.9, 125.1, 123.8, 121.6, 120.3; ESI-MS (*m*/*z*, %): 265.09 (60).

*4-Oxo-2-(p-tolyl)quinazoline-3(4H)-carboxamide (**VIc**)*

Yield: 50%; mp: 310–312°C; ^{1}H NMR (DMSO-d_6) δ ppm: 3.24 (s, 3H, CH_3), 5.73 (s, 2H, $-NH_2$), 7.28–8.4 (m, 8H, Ar–H); ^{13}C NMR (DMSO-d_6) δ: 179.3, 178.1, 143.5, 138.7, 136.3, 135.1, 133.4, 129.3, 127.1, 125.9, 124.3, 123.6, 121.5, 28.1; ESI-MS (*m*/*z*, %): 279.10 (80).

Ullmann condensation [17]

To a mixture of *o*-chloro benzoic acid (0.05 moles), anthranilic acid (0.05 moles) and copper powder (0.2 g) in 60 mL of isoamylalcohol, 5 g of dry potassium carbonate was slowly added. The above reaction mixture was allowed to reflux for 6–8 h on an oil bath. After completion of the reaction as evidenced by TLC, isoamylalcohol was removed under steam distillation. The mixture was poured into one liter of hot water and acidified with concentrated hydrochloric acid. The resulting precipitate was collected by filtration, and washed with hot water. The crude acid was dissolved in aqueous sodium hydroxide solution, boiled in the presence of activated charcoal and filtered. On acidification of the filtrate with concentrated hydrochloric acid, light yellowish precipitate was obtained which was washed with hot water and recrystallized from aqueous methanol to give light yellow product 2,2′-iminodibenzoic acid (**C**). Yield: 91%, mp: 187°C.

*Synthesis of acridone-4-carboxylic acid (**D**) [16]*

Five grams of 2,2′-iminodibenzoic acid (**C**) was taken into a round bottom flask and 50 g of polyphosphoric acid was added and the reaction mixture was shaken well and heated at 100°C for 3 h. Appearance of yellow color indicated the completion of the reaction. Then, it was poured into hot water and made alkaline by ammonia. The yellow precipitate obtained was filtered and collected. The acridone-4-carboxylic acid (**D**) was recrystallized from acetic acid.

Yield 69%; mp: 326–328°C; ^{1}H NMR (DMSO-d_6) δ ppm: 7.29–8.48 (m, 7H, Ar–H), 11.23 (s, 1H, NH), 12.68 (s, 1H, OH); ^{13}C NMR (DMSO-d_6) δ: 178.4, 158.3, 139.5, 138.2, 133.5, 131.9, 129.5, 128.5, 125.4, 124.3, 123.4, 120.9; ESI-MS (*m*/*z*, %): 239.01 (100).

*General method for the synthesis of N-(2-methyl-4-oxoquinazolin-3(4H)-yl)-9-oxo-9,10-dihydroacridine-4-carboxamide (**1**)*

To the suspension of acridone (2.09 mmol) in 15 mL of dry toluene, thionyl chloride (2.90 mmoles) and dry pyridine (2.90 mmoles) were added. The reaction mixture was stirred at room temperature for about 3–4 h. Then the resulting reaction mixture was mixed with3-amino-2-methylquinazolin-4(3*H*)-one (**IVa**) (2.09 mmoles), triethylamine (6.185 mmoles) and stirred for another 3 h, reaction was monitored by TLC. After completion of the reaction, the solvent was removed under vacuum, resulted crude reaction mixture was poured into ice cold water to get solid residue. The precipitate was filtered, washed with water and dried. The crude product was recrystallized from methanol.

Yield 59%; mp: 172–174°C; ^{1}H NMR (DMSO-d_6) δ ppm: 2.34 (s, 3H, CH_3), 6.91–8.31 (m, 11H, Ar–H), 9.23 (s, 1H, CONH), 11.61 (s, 1H, NH); ^{13}C NMR (DMSO-d_6) δ: 178.5, 176.2, 168.7, 145.6, 144.3, 142.4, 139.3, 138.7, 135.4, 133.5, 132.4, 129.5, 128.5, 125.4, 124.3, 123.4, 122.3, 120.9, 119.5, 23.5; ESI-MS (*m*/*z*, %): 396.12 (76); Anal.

calcd. for $C_{23}H_{16}N_4O_3$: C-69.69, H-4.07, N-14.13; Found: C-69.38, H-3.78, N-13.91.

*N-(4-Oxo-2-phenylquinazolin-3(4H)-yl)-9-oxo-9,10-dihydroacridine-4-carboxamide (**2**)*

Yield 48%;mp: 165–167°C; ^{1}H NMR (DMSO-d_6) δ ppm: 7.33–8.54 (m, 16H, Ar–H), 9.11 (s, 1H, NHCO), 11.6 (s, 1H, NH); ^{13}C NMR (DMSO-d_6) δ: 177.4, 176.6, 167.4, 146.4, 144.7, 143.9, 141.8, 139.8, 138.6, 137.5, 136.9, 134.6, 132.8, 129.2, 127.8, 126.7, 126.4, 124.1, 124.9, 123.4, 122.3, 120.9, 119.5, 118.6, 117.4; ESI-MS (*m*/*z*, %): 458.14 (30); Anal. calcd. for $C_{28}H_{18}N_4O_3$: C-73.35, H-3.96, N-12.22; Found: C-73.04, H-3.66, N-12.01.

*N-(4-Oxo-2-(p-tolyl)quinazolin-3(4H)-yl)-9-oxo-9,10-dihydroacridine-4-carboxamide (**3**)*

Yield 51%; mp: 274–277°C; ^{1}H NMR (DMSO-d_6) δ ppm: 2.37 (s, 3H, CH_3), 7.33–8.55 (m, 15H, Ar–H), 9.21 (s, 1H, NHCO), 11.38 (s, 1H, NH); ^{13}C NMR (DMSO-d_6) δ: 178.4, 176.6, 168.4, 146.7, 144.5, 143.4, 142.7, 141.6, 140.4, 138.6, 136.9, 134.6, 132.8, 129.2, 127.8, 126.7, 126.4, 124.1, 124.9, 123.4, 122.3, 120.9, 119.5, 118.6, 117.4, 28.9; ESI-MS (*m*/*z*, %): 472.15 (70); Anal. calcd. for $C_{29}H_{20}N_4O_3$: C-73.72, H-4.27, N-11.86; Found: C-73.40, H-3.98, N-11.65.

*N-[(2-Methyl-4-oxo-3,4-dihydroquinazoline-3-carbonothioyl)-9-oxo-9,10-dihydroacridine-4-carboxamide (**4**)*

Yield 45%; mp: 204–206°C; ^{1}H NMR (DMSO-d_6) δ ppm: 2.35 (s, 3H, CH_3), 6.91–8.37 (m, 11H, Ar–H), 9.23 (s, 1H, NHCO), 11.34 (s, 1H, NH); ^{13}C NMR (DMSO-d_6) δ: 179.7, 178.2, 176.2, 164.6, 147.8, 143.1, 142.4, 141.5, 139.1, 138.4, 137.2, 135.3, 134.3, 129.4, 128.4, 127.8, 126.7, 125.4, 124.7, 122.7, 120.2. 23.5; ESI-MS (*m*/*z*, %): 440.09; Anal. calcd. for $C_{24}H_{16}N_4O_3S$: C-65.44, H-3.66, N-12.72; Found: C-65.12, H-3.37, N-12.51.

*N-(4-Oxo-2-phenyl-3,4dihydroquinazoline-3-carbonothioyl)-9-oxo-9,10-dihydroacridine-4-carboxamide (**5**)*

Yield 35%; mp: 178–181°C; ^{1}H NMR (DMSO-d_6) δ ppm: 7.18–8.38 (m, 16H, Ar-H), 9.13 (s, 1H, NHCO), 11.23 (s, 1H, NH); ^{13}C NMR (DMSO-d_6) δ: 179.1, 173.3, 168.3, 167.3, 143.3, 142.8, 141.2, 139.6, 138.2, 136.6, 135.2, 134.2, 132.4, 130.5, 129.6, 128.6, 127.2, 126.5, 125.8, 124.7, 123.3, 121.3, 120.2, 119.4, 118.6, 117.8; ESI-MS (*m*/*z*, %): 502.11 (65); Anal. calcd. for $C_{29}H_{18}N_4O_3S$: C-69.31, H-3.61, N-11.15; Found: C-69.02, H-3.07, N-10.94.

*N-(4-Oxo-2-(p-tolyl)-3,4-dihydroquinazoline-3-carbonothioyl)-9-oxo-9,10-dihydroacridine-4-carboxamide (**6**)*

Yield 37%; mp: 288–290°C; ^{1}H NMR (DMSO-d_6) δ ppm: 2.39 (s, 3H, CH_3), 6.85–8.33 (m, 15H, Ar–H), 9.23 (s, 1H, NHCO), 11.63 (s, 1H, NH); ^{13}C NMR (DMSO-d_6) δ: 179.2, 176.1, 171.3, 168.3, 146.7, 145.2, 143.3, 142.8, 141.2, 139.6, 138.2, 136.6, 135.2, 134.2, 132.4, 130.5, 129.4, 128.4, 127.8, 126.7, 125.4, 124.7, 122.7, 120.2, 119.2, 118.2, 117.8, 25.1; ESI-MS (*m*/*z*, %): 516.13 (80); Anal. calcd. for $C_{30}H_{20}N_4O_3S$: C-69.75, H-3.90, N-10.85; Found: C-69.44, H-3.59, N-10.62.

*N-[(2-Methyl-4-oxo-3,4-dihydroquinazoline-3-carbonyl)-9-oxo-9,10-dihydroacridine-4-carboxamide (**7**)*

Yield 64%; mp: 182–185°C; ^{1}H NMR (DMSO-d_6) δ ppm: 2.32 (s, 3H, CH_3), 6.91–8.37 (m, 11H, Ar–H), 10.23 (s, 1H, NHCO), 11.56 (s, 1H, NH); ^{13}C NMR (DMSO-d_6) δ: 179.7, 174.6, 168.3, 166.3, 142.8, 141.7, 139.4, 136.8, 134.2, 132.4, 130.5, 129.4, 128.4, 126.7, 124.7, 122.7, 121.3, 120.2, 119.2, 118.2, 117.8, 28.9; ESI-MS (*m*/*z*, %): 424.12 (75); Anal. calcd. for $C_{24}H_{16}N_4O_4$: C-67.92, H-3.80, N-13.20; Found: C-67.62, H-3.51, N-12.97.

*N-(4-Oxo-2-phenyl-3,4-dihydroquinazoline-3-carbonyl)-9-oxo-9,10-dihydroacridine-4-carboxamide (**8**)*

Yield 38%; mp: 147–149°C; ^{1}H NMR (DMSO-d_6) δ ppm: 7.15–8.37 (m, 16H, Ar–H), 9.33 (s, 1H, NHCO), 11.91 (s, 1H, NH); ^{13}C NMR (DMSO-d_6) δ: 179.3, 174.7, 168.5, 165.3, 143.3, 142.8, 141.2, 139.6, 138.2, 136.6, 135.5, 134.3, 132.6, 130.7, 129.4, 128.6, 127.8, 126.7, 125.4, 124.7, 122.7, 121.3, 120.2, 119.2, 118.2, 117.8; ESI-MS (*m*/*z*, %): 486.13 (65); Anal. calcd. for $C_{29}H_{18}N_4O_4$: C-71.60, H-3.73, N-11.52; Found: C-71.31, H-3.43, N-11.31.

*N-(4-Oxo-2-(p-tolyl)-3,4-dihydroquinazoline-3-carbonyl)-9-oxo-9,10-dihydroacridine-4-carboxamide (**9**)*

Yield 41%; mp: 267–269°C; ^{1}H NMR (DMSO-d_6) δ ppm: 2.39 (s, 3H, CH_3), 7.12–8.23 (m, 15H, Ar–H), 9.29 (s, 1H, NHCO), 11.87 (s, 1H, NH); ^{13}C NMR (DMSO-d_6) δ: 179.6, 173.3, 167.3, 165.4, 144.5, 143.8, 141.5, 139.6, 138.5, 137.3, 135.6, 134.3, 133.4, 131.5, 129.3, 128.7, 127.6, 126.3, 125.6, 123.7, 122.4, 121.7, 120.5, 119.6, 118.3, 117.6, 29.5; ESI-MS (*m*/*z*, %): 500.15 (45); Anal. calcd. for $C_{30}H_{20}N_4O_4$: C-71.99, H-4.03, N-11.19; Found: C-71.67, H-3.73, N-10.97.

*N-(6-Iodo-2-methyl-4-oxoquinazolin-3(4H)-yl)-9-oxo-9,10-dihydroacridine-4-carboxamide (**10**)*

Yield 55%; mp: 180–182°C; ^{1}H NMR (DMSO-d_6) δ ppm: 2.34 (s, 3H, CH_3), 6.91–8.31 (m, 10H, Ar–H), 9.23 (s, 1H, CONH), 11.41 (s, 1H, NH); ^{13}C NMR (DMSO-d_6) δ: 178.3, 176.9, 168.1, 145.7, 144.3, 141.4, 139.3, 138.7, 136.4, 133.1, 132.6, 129.7, 128.3, 125.4, 124.3, 123.6, 122.7, 121.9, 119.3, 23.3; ESI-MS (*m*/*z*, %): 523.29 (76); Anal. calcd. for $C_{23}H_{15}IN_4O_3$: C-52.89, H-2.89, N-10.73; Found: C-52.57, H-2.57, N-10.51.

*N-[(6-Iodo-2-methyl-4-oxoquinazolin-3(4H)-yl)carbonyl]-9-oxo-9,10-dihydroacridine-4-carboxamide (**16**)*

Yield 70%; mp: 180–182°C; ^{1}H NMR (DMSO-d_6) δ ppm: 2.32 (s, 3H, CH_3), 6.91–8.37 (m, 10H, Ar–H), 10.23 (s, 1H, NHCO), 11.56 (s, 1H, NH); ^{13}C NMR (DMSO-d_6) δ: 179.3, 177.6, 168.7, 166.9, 142.3, 141.7, 139.1, 136.3, 135.2, 132.4, 130.3, 129.4, 128.3, 126.7, 124.1, 122.7, 121.3, 120.2, 119.3, 118.2, 117.8, 28.7; ESI-MS (*m*/*z*, %): 551.3 (75); Anal. calcd. for $C_{24}H_{15}IN_4O_4$: C-52.38, H-2.75, N-10.18; Found: C-52.37, H-2.43, N-9.97.

*N-(6-Bromo-2-methyl-4-oxoquinazolin-3(4H)-yl)-9-oxo-9,10-dihydroacridine-4-carboxamide (**19**)*

Yield 51%; mp: 170–172°C; ^{1}H NMR (DMSO-d_6) δ ppm: 2.34 (s, 3H, CH_3), 6.91–8.31 (m, 10H, Ar–H), 9.23 (s, 1H, CONH), 11.51 (s, 1H, NH); ^{13}C NMR (DMSO-d_6) δ: 178.2, 176.1, 168.3, 145.9, 144.4, 142.1, 139.3, 137.7, 136.4, 133.1, 132.3, 129.5, 128.3, 125.1, 124.3, 123.7, 122.3, 120.3, 119.6, 23.7; ESI-MS (*m*/*z*, %): 476.2 (76); Anal. calcd. for $C_{23}H_{15}BrN_4O_3$: C-58.12, H-3.18, N-11.70; Found: C-57.80, H-2.86, N-11.47.

*N-[(6-Bromo-2-methyl-4-oxoquinazolin-3(4H)-yl)-carbonyl]-9-oxo-9,10-dihydroacridine-4-carboxamide (**25**)*

Yield 65%; mp: 188–190°C; ^{1}H NMR (DMSO-d_6) δ ppm: 2.32 (s, 3H, CH_3), 6.91–8.37 (m, 10H, Ar–H), 10.23 (s, 1H, NHCO), 11.56 (s, 1H, NH); ^{13}C NMR (DMSO-d_6) δ: 179.5, 176.6, 168.7, 166.9, 142.3, 141.7,

139.7, 136.3, 134.9, 132.6, 130.5, 129.4, 128.4, 126.3, 124.9, 122.6, 121.5, 120.3, 119.7, 118.2, 117.3, 28.3; ESI-MS (*m*/*z*, %): 504.3 (75); Anal. calcd. for $C_{24}H_{15}BrN_4O_4$: C-57.27, H-3.00, N-11.13; Found: C-56.96, H-2.71, N-10.92.

Pharmacology

In vitro cytotoxic studies by SRB assay

The acridone tagged quinazolinone derivatives were evaluated for cytotoxicity against different cancer cells (MCF7, LS174T, SW1398, and WiDr) by using the sulforhodamine B (SRB) [18]. In brief, cells were cultured in RPMI 1640 supplemented with 10% fetal calf serum, and cultures were passed once or twice a week using trypsin EDTA to detach the cells from their culture flasks. The fast growing cells were harvested, counted, and plated at suitable concentrations in 96-well micro plates. After incubation for 24 h, the compounds dissolved in the culture medium were added to the culture wells in triplicate and incubated further for 72 h at 37°C under 5% CO_2 atmosphere. One separate plate was used to determine the number of cells at the moment of drug addition. This plate was immediately fixed. The other cultures were fixed at 72 h with cold TCA and stained with 0.4% SRB dissolved in 1% acetic acid. After dissolving the bound stain with 150 μl of 10 mM unbuffered Tris base (Tris (hydroxyl methyl) amino methane) solution using gyratory shaker, absorbance was measured at 540 nm using a microplate reader (Tecan). The cytotoxicity was assessed by measuring the concentration required to inhibit protein synthesis by 50% (i.e. IC_{50}) as comparison. Each value represents the mean of triplicate experiments.

In vitro inhibition of EGFR tyrosine kinase

The EGFR tyrosine kinase inhibition assay was performed by using Kinase-Glo Plus luminescence kinase assay kit. In this method, kinase activity was determined by quantitating the amount of ATP remaining in solution of a kinase reaction [19]. The luminescent signal from the assay is correlated with the amount of ATP present and it was inversely related with kinase activity. The compounds were diluted to 100 mM in 10% DMSO and 5 mL of the dilution was added to a 50 mL reaction. All of the enzymatic reactions were conducted at 30°C for 40 min, 50 mL of reaction mixture contains 10 mM $MgCl_2$, 40 mM Tris, pH 7.4, 0.1 mg/mL BSA, 0.2 mg/mL Poly (Glu, Tyr) substrate, 10 mM ATP and EGFR. After the enzymatic reaction, 50 mL of Kinase-GloPlus Luminescence kinase assay solution was added to each reaction and incubate the plate for 5 min at room temperature. The protein kinase assays used to determine IC_{50} value were performed using ADP-Glo assay kit, which measures the generation of ADP by the protein kinase. Generation of ADP by the protein kinase reaction leads to an increase in luminescence signal in the presence of ADP-Glo assay kit. The assay was started by incubating the reaction mixture in a 96-well plate at 30°C for 30 min. After the 30 min incubation period, the assay was terminated by the addition of 25 mL of ADP-Glo reagent. The 96-well plate was shaken and then incubated for 30 min at ambient temperature. Then, 50 mL of kinase detection reagent was added, the 96-well reaction plate was then read using the ADP-Glo Luminescence reader. Blank control was set up that included all the assay components except the addition of appropriate substrate. The corrected activity for each protein kinase target was determined by removing the blank control value.

Molecular docking studies

Initially a digital structure of the target kinase domain of EGFR was retrieved from the Protein databank website with PDB Id: 1M17. Protein structure optimization was done by using Protein preparation wizard, which corrects the protein structure by adding hydrogen's to satisfy the valences and optimized by using OPLS-2005 force field (optimized potentials for liquid simulations) [20].

Protein ligand interactions were examined by using Glide XP docking protocol, which includes two basic steps, Receptor Grid generation and ligand docking. Previous X-ray crystallographic studies of the EGFR complex revealed the binding site components and a grid was generated considering the volume of the active binding pocket of the protein. Each ligand was docked in to the active site of the target protein using XP mode of Glide. Glide Score includes a steric-clash term, adds polar terms featured by Schrodinger to correct electrostatic mismatches [21–24]. Glide score is a combination of hydrophilic, hydrophobic, metal binding groups, Van der Waals energy, freezing rotatable bonds, and polar interactions with receptor.

V.V.S.R.P. would like to gratefully acknowledge All India Council for Technical Education (AICTE), Government of India for "Career Award for Young Teachers" (CAYT) and research grant (1-51/RIFD/CA/11/2011-12). The authors would like to acknowledge the Laboratory Medical Oncology, VU University Medical Center, Amsterdam, The Netherlands for providing necessary research facilities to carry out the cytotoxicity studies.

The authors have declared no conflict of interest.

References

[1] G. P. Zambetti, *J. Cell Physiol.* **2007**, *213*, 370–373.
[2] A. Harlozinska, *Anticancer Res.* **2005**, *25*, 3327–3333.
[3] L. Kopfstein, G. Christofori, *Cell Mol. Life. Sci.* **2006**, *63*, 449–468.
[4] F. Ciardiello, G. Tortora, *Clin. Cancer Res.* **2001**, *7*, 2958–2970.
[5] G. Viktor, H. Manuel, *J. Natl. Cancer Inst.* **2003**, *95*, 851–867.
[6] S. Ménard, P. Casalini, M. Campiglio, S. M. Pupa, E. Tagliabue, *Cell. Mol. Life. Sci.* **2004**, *61*, 2965.
[7] E. Galvani, G. J. Peters, E. Giovannetti, *Future Oncology* **2012**, *8*, 1015–1029.
[8] S. Madhusudan, T. S. Ganesan, *Clin. Biochem.* **2004**, *37*, 618–635.
[9] G. S. Cockerill, K. E. Lackey, *Curr. Top. Med. Chem.* **2002**, *2*, 1001–1010.
[10] Y. C. Mayur, G. J. Peters, V. V. S. Rajendra Prasad, C. Lemos, N. K. Sathish, *Curr. Cancer Drug Targets* **2009**, *9*, 298–306.
[11] G. Krishnegowda, P. Thimmaiah, R. Hegde, C. Dass, P. J. Houghton, K. N. Thimmaiah, *Bioorg. Med. Chem.* **2002**, *10*, 2367–2380.
[12] V. V. S. Rajendra Prasad, J. Venkatrao, R. S. Giri, N. K. Satish, S. M. Shanta Kumar, Y. C. Mayur, *Chemico. Biol. Inter.* **2008**, *176*, 212–219.

[13] V. V. S. Rajendra Prasad, G. J. Peters, C. Lemos, I. Kathmann, Y. C. Mayur, *Eur. J. Pharm. Sci.* **2011**, *43*, 217–224.

[14] V. V. S. Rajendra Prasad, G. Deepak Reddy, D. Appaji, G. J. Peters, Y. C. Mayur, *J. Mol. Graph. Mod.* **2013**, *40*, 116–124.

[15] N. Malleshappa, M. Noolvi, B. Harun Patel, C. Varun, C. Ankit, *Eur. J. Med. Chem.* **2011**, *46*, 2327–2346.

[16] A. S. El-Azab, M. A. Al-Omar, A. A. Abdel-Aziz, N. I. Abdel-Aziz, M. A. el-Sayed, A. M. Aleisa, M. M. Sayed-Ahmed, S. G. Abdel-Hamide, *Eur. J. Med. Chem.* **2010**, *45*, 4188–4198.

[17] H. Weingarten, *J. Org. Chem.* **1964**, *29*, 3624–3626.

[18] Y. Keepers, P. E. Pizao, G. J. Peters, J. Van Ark-Otte, B. Winograd, H. M. Pinedo, *Eur. J. Cancer* **1991**, *27*, 897–900.

[19] D. Balzano, S. Santaguida, A. Musacchio, F. Villa, *Chem. Biol.* **2011**, *18*, 966–975.

[20] Schrodinger Suite, Protein Preparation Wizard, Schrödinger, 2012, LLC, New York.

[21] R. A. Friesner, J. L. Banks, R. B. Murphy, T. A. Halgren, J. J. Klicic, D. T. Mainz, M. P. Repasky, E. H. Knoll, D. E. Shaw, M. Shelley, J. K. Perry, P. Francis, P. S. Shenkin, *J. Med. Chem.* **2004**, *47*, 1739–1749.

[22] R. A. Friesner, R. B. Murphy, M. P. Repasky, L. L. Frye, J. R. Greenwood, T. A. Halgren, P. C. Sanschagrin, D. T. Mainz, *J. Med. Chem.* **2006**, *49*, 6177–6196.

[23] T. A. Halgren, R. B. Murphy, R. A. Friesner, H. S. Beard, L. L. Frye, W. T. Pollard, J. L. Banks, *J. Med. Chem.* **2004**, *47*, 1750–1759.

[24] Schrodinger Suite, Glide, Schrodinger, 2012, LLC, New York.

